

Accurate determination of anisotropic thermal conductivity for ultrathin composite film

Qiu-Hao Zhu(朱秋毫), Jing-Song Peng(彭景淞), Xiao Guo(郭潇), Ru-Xuan Zhang(张如轩), Lei Jiang(江雷), Qun-Feng Cheng(程群峰), and Wen-Jie Liang(梁文杰)

Citation: Chin. Phys. B, 2022, 31 (**10**): 108102. DOI: 10.1088/1674-1056/ac6ee5
Journal homepage: http://cpb.iphy.ac.cn; http://iopscience.iop.org/cpb

What follows is a list of articles you may be interested in

High-quality CdS quantum dots sensitized ZnO nanotube array films for superior photoelectrochemical performance

Qian-Qian Gong(宫倩倩), Yun-Long Zhao(赵云龙), Qi Zhang(张奇), Chun-Yong Hu(胡春永), Teng-Fei Liu(刘腾飞), Hai-Feng Zhang(张海峰), Guang-Chao Yin(尹广超)[†], and Mei-Ling Sun(孙美玲)[‡]
Chin. Phys. B, 2022, 31 (**9**): 098103. DOI: 10.1088/1674-1056/ac4cc2

Enhancing the thermoelectric performance through the mutual interaction between conjugated polyelectrolytes and single-walled carbon nanotubes

Shuxun Wan(万树勋), Zhongming Chen(陈忠明), Liping Hao(郝丽苹), Shichao Wang(王世超), Benzhang Li(李本章), Xiao Li(黎潇), Chengjun Pan(潘成军), and Lei Wang(王雷)
Chin. Phys. B, 2022, 31 (**2**): 028104. DOI: 10.1088/1674-1056/ac48f9

Thermoelectric characteristics of flexible reduced graphene oxide/silver selenide nanowire composites prepared by a facile vacuum filtration process

Zuo Xiao(肖佐), Yong Du(杜永), Qiufeng Meng(孟秋风), and Lei Wang(王磊)
Chin. Phys. B, 2022, 31 (**2**): 028103. DOI: 10.1088/1674-1056/ac447e

Ultra-wideband circular-polarization converter with micro-split Jerusalem-cross metasurfaces

Xi Gao(高喜), Xing-Yang Yu(余行阳), Wei-Ping Cao(曹卫平), Yan-Nan Jiang(姜彦南), Xin-Hua Yu(于新华)
Chin. Phys. B, 2016, 25 (**12**): 128102. DOI: 10.1088/1674-1056/25/12/128102

Characterization of atomic-layer MoS_2 synthesized using a hot filament chemical vapor deposition method

Ying-Zi Peng(彭英姿), Yang Song(宋扬), Xiao-Qiang Xie(解晓强), Yuan Li(李源), Zheng-Hong Qian(钱正洪), Ru Bai(白茹)
Chin. Phys. B, 2016, 25 (**5**): 058104. DOI: 10.1088/1674-1056/25/5/058104

Accurate determination of anisotropic thermal conductivity for ultrathin composite film

Qiu-Hao Zhu(朱秋毫)[1,2], Jing-Song Peng(彭景淞)[3], Xiao Guo(郭潇)[1,2,4], Ru-Xuan Zhang(张如轩)[1], Lei Jiang(江雷)[3], Qun-Feng Cheng(程群峰)[3,†], and Wen-Jie Liang(梁文杰)[1,2,4,‡]

[1] *Beijing National Center for Condensed Matter Physics, Beijing Key Laboratory for Nanomaterials and Nanodevices, Institute of Physics, Chinese Academy of Sciences (CAS), Beijing* 100190, *China*

[2] *CAS Center of Excellence in Topological Quantum Computation and School of Physical Sciences, University of Chinese Academy of Sciences, Beijing* 100190, *China*

[3] *School of Chemistry, Key Laboratory of Bio-inspired Smart Interfacial Science and Technology of Ministry of Education, Beijing Advanced Innovation Center for Biomedical Engineering, Beihang University, Beijing* 100191, *China*

[4] *Songshan Lake Materials Laboratory, Dongguan* 523808, *China*

(Received 18 March 2022; revised manuscript received 30 April 2022; accepted manuscript online 12 May 2022)

Highly anisotropic thermal conductive materials are of significance in thermal management applications. However, accurate determination of ultrathin composite thermal properties is a daunting task due to the tiny thermal conductance, severely hindering the further exploration of novel efficient thermal management materials, especially for size-confined environments. In this work, by utilizing a hybrid measuring method, we demonstrate an accurate determination of thermal properties for montmorillonite/reduced graphene oxide (MMT/rGO) composite film with a thickness range from 0.2 μm to 2 μm. The in-plane thermal conductivity measurement is realized by one-dimensional (1D) steady-state heat conduction approach while the cross-plane one is achieved via a modified 3ω method. As-measured thermal conductivity results are cross-checked with different methods and known materials, revealing the high measurement accuracy. A high anisotropic ratio of 60.5, independent of composite thickness, is observed in our measurements, further ensuring the negligible measurement error. Notably, our work develops an effective approach to the determination of ultrathin composite thermal conductivity, which may promote the development of ultrathin composites for potential thermal-related applications.

Keywords: ultrathin, composite film, thermal conductivity, anisotropic ratio

PACS: 81.70.–q, 68.65.Ac, 81.05.U–, 65.40.G– **DOI:** 10.1088/1674-1056/ac6ee5

1. Introduction

With the further miniaturization of transistors, more and more devices are integrated into a single integrated circuit chip. Owing to the consequent large power density, local overheating becomes a great challenge if the heat dissipation capability is poor. High temperature will severely degrade the system performance because of thermal fluctuation effects, and also cause a great many of irreversible damages to the inner devices and sensing units, thus accelerating their aging processes. Thus, efficient thermal management is of great importance in the field of chip manufacturing and packaging.[1,2] Films with highly anisotropic thermal conductivity whose in-plane thermal conductivity (λ_x) is substantially higher than the cross-plane one (λ_z),[3,4] capable of in-plane rapid Joule heat diffusion and out-of-plane thermal heat blocking, have attracted extensive research interest in the past few decades.[5,6] It is a promising way to realize high-performance on-chip systems with a long-duration stability by directionally accelerating heat transfer that depositing such films on chip surface within a limited space, which have the capacity to conduct heat from local overheating spots, ensuring that the other internal structures are not susceptive to adjacent thermal fields. Hence, the exploration of ultrathin (< 10 μm) thermal management films is of great value for the applications in some specific size-confined environments. However, the accurate determination of thermal conductivity for ultrathin composite film is still a pending issue due to its ultrathin nature and small thermal conductance; hence, now there are no reports on ultrathin (micron-sized) composite films for efficient thermal management.

Usually, in-plane and cross-plane thermal conductivity λ_x and λ_z of thick composite film are determined by using laser flash techniques by heating the films in the center with a laser pulse and measuring its in-/cross-plane thermal response (surface temperatures) at the edge/rear with an infrared detector.[7–10] However, this method is in question for the thermal property measurement of ultrathin composite films.[11] For cross-plane measurements, on the one hand, ultrathin film reaches a thermal equilibrium state in the cross-plane direction within a very short time, and visible temperature difference could be hardly obtained. Hence, fitted and extracted thermal diffusivity is unreliable. On the other hand, the laser penetration depth is comparable or larger in ultrathin films, making the adopted 1D cross-plane heat diffusion

†Corresponding author. E-mail: cheng@buaa.edu.cn
‡Corresponding author. E-mail: wjliang@iphy.ac.cn

© 2022 Chinese Physical Society and IOP Publishing Ltd

model invalid. As for in-plane measurements, the direct contact of sample holder's cap mask to film surface dramatically affects the in-plane thermal transport process from the laser-heated spot to the detector-sensed one for ultrathin composite with small thermal conductance, raising the measurement error. Some other typical measurement methods, including Raman method,[12,13] 3ω method,[14,15] and suspension bridge method,[16,17] are also proposed to detect thin film in-plane thermal conductivity. Nevertheless, the small laser penetration depth, unmatched heat penetration depth or large thermal contact resistance drastically rigidify the boundary conditions, limiting their practical applications in our micron-sized ultrathin composite film measurements.

To accurately determinate the highly anisotropic thermal conductivity of ultrathin composite film with a thickness less than 10 μm, we develop a hybrid method combining the 1D steady-state heat conduction approach and the 3ω method in this work. We carry out measurements based on a montmorillonite/reduced graphene oxide (MMT/rGO) composite system, and the measurement accuracy is verified by control experiments. A more reliable λ_x result of ~ 3.99 W·m^{-1}·K^{-1} is obtained through the modified 1D steady-state means by effectively eliminating the influence from background heat dissipation and contact thermal resistance. On the other hand, a reduced λ_z value of ~ 0.066 W·m^{-1}·K^{-1} and a high anisotropic ratio of ~ 60.5 are discovered for composite films by using the 3ω method through avoiding the laser penetration effects. As-measured composite thermal conductivity is independent of film thickness from 0.2 μm to 2 μm, further attesting the feasibility of our measurement method.

2. Results and discussion

2.1. Material characterization

The multi-layered composite film to be tested is synthesized through layer-by-layer filtration with a mixture of MMT and rGO layers (in Fig. 1(a)). Total thickness of ultrathin hybrid film, ranging from ~ 0.2 μm to 2 μm, is related to the deposition cycle (n, 1–10). A typical cross-sectional scanning electron microscopy (SEM) image of the film (Fig. 1(b)) shows that the MMT/rGO layers are stacked along the cross-plane direction, corresponding with our measurement requirements for highly-anisotropic thermal conductive material. The x-ray diffraction (XRD) patterns show the crystallographic structure of the as-prepared composite as shown in Fig. 1(c), where five distinct peaks exist in the spectra. An evident diffraction peak centered at 6.7° possesses a high intensity, corresponding to (001) plane for MMT in the composite. Two small high-order peaks detected at 13.4° and 19.7°, corresponding to (002) and (020) planes of MMT, further attest its short-range order nature. The d-spacing value for MMT(001) plane is ~ 13.18 Å in the stack composite, similar to the value reported previously.[18] Two characteristic peaks at 26.6° and 44.7° (Fig. 1(c)) are from (002) plane and 2D (10) plane of rGO layer. The calculated d-spacing value of ~ 3.35 Å for 26.6° peak matches ideally with that of graphite (002) plane.[19,20] We see no other impurity phases from our XRD patterns, indicating that the composite only consists of MMT and rGO.

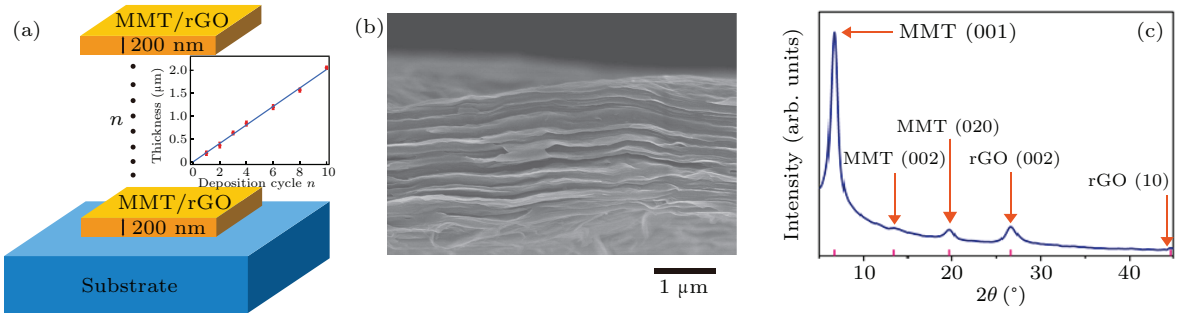


Fig. 1. (a) Schematic illustration for film composition and measured film thickness. (b) Cross-sectional SEM image of $(MMT/rGO)_{15}$ composite film, and (c) XRD pattern of the film.

2.2. In-plane thermal conductivity measurement

We adopt an improved 1D steady-state heat conduction method, *i.e.* using a four-probe configuration under a high-vacuum condition to measure λ_x at room temperature, which is a more essential and reliable method.[21,22] The steady-state measurement system (Fig. 2(a)) is carried out in a probe station's vacuum chamber. A heat flow is generated by a suspended resistive heater at the hot junction, passes through a narrow and long strip composite sample (cut from the MMT/rGO composite film) and is absorbed by a copper block at the clod junction. Two thermocouples are connected with a hot end and a cold end respectively to measure the corresponding hot-/cold-junction temperature T_h and T_c. Our sample strips are suspended and glued with silver paste between the two junctions. Strip length (l) and width (w) are ~ 2 mm and ~ 1 mm, respectively, and its thickness (h) is variable in our experiments. To minimize the influence of inevitable background heat losses, including the radiation and the heat flow from supporting structures, thermal conductance of ten composite strips is measured together to enhance thermal conductance signal. At the same time, hot junction is completely supported by the pull of thin insulated constantan wires.

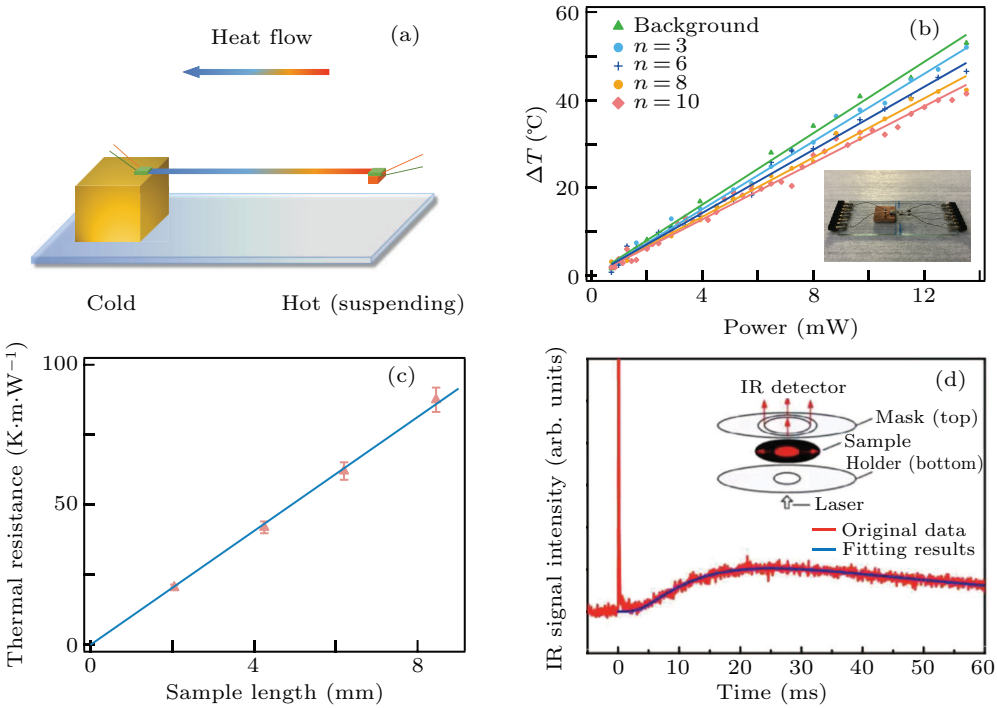


Fig. 2. (a) A schematic illustration for modified four-probe setup. (b) Temperature differences between two junctions as a function of heating power for samples with various values of deposition cycle n, with inset showing actual measurement setup. (c) Measured total thermal resistance as a function of sample strip length. (d) Measured IR signal intensity *versus* time for $(MMT/rGO)_5$ composite by laser flash technique.

Figure 2(b) shows the in-plane thermal conductance measurement results for composite strips with different values of n. The background heat dissipation is also exhibited. Note that the background signal is obtained when no sample is suspended on the two junctions, and it is completely determined by heat leakages through the thermocouples and conduction wires together with radiation heat loss. It is found that the temperature difference between two junctions ($\Delta T = T_h - T_c$) shows an approximately linear dependence on the heating power, and there appear obvious ΔT differences between various samples. The film thermal conductance (G) can be determined by the difference between the reciprocals of fitted slopes for the tested structure and the background. According to the relationship $\lambda_x = Gl/wh$, the values of the in-plane thermal conductivity λ_x are obtained to be 4.04, 4.00, 4.07, and 3.84 W·m^{-1}·K^{-1} for strip samples with a deposition cycle of 3, 6, 8, and 10, respectively. Hence, it shows that λ_x remains constant when the sample thickness changes, indicating the accuracy and reliability of the measurement. To estimate the thermal contact resistances at hot junction and cold junction and to guarantee our thermal measurement accuracy, the thermal resistances of samples are repeatedly measured for strips with the same thickness (~ 2 μm) and different lengths. As illustrated in Fig. 2(c), there exists an approximately linear relationship between the measured total thermal resistance and the strip length for multiple measurements, and the linear fitting result passes through the origin within an allowed error range. Thus, it indicates that the total thermal contact resistance is negligible and has little influence on the measured values of λ_x.

As stated above, the conventional laser flash technique is not suitable for measuring the thermal conductances of ultrathin films. To the best of our knowledge, the film thickness of the thinnest composite that was measured by using this technique is on the order of 10 μm to 100 μm.[23–27] For comparison, we also try to estimate in-plane thermal conductivity of ultrathin (~ 1 μm) $(MMT/rGO)_5$ film by using the laser flash technique. Not surprisingly, either the signal is too small to be detected, or laser irradiation creates local heating and makes visual damage to the thin samples. One of such measurement results is shown in Fig. 2(d). The in-plane thermal diffusion coefficient and thermal conductivity of the extracted composite are 177.0 ± 14.7 mm^2·s^{-1} and ~ 442.5 W·m^{-1}·K^{-1}, respectively, even greatly exceeding the reported values of pure rGO materials,[4] indicating the large potential measurement errors for in-plane thermal measurements of thin composites. This may be due to the inevitable large thermal leakage induced by laser flash measurement setup, where the cap mask of sample holder closely contacts the film surface as shown in the inset.

It is noted that although the sample will keep a better balance assisted by supporting the hot junction with a nylon wire (see the inset of Fig. 3(a)), the background thermal conductance reaches up to 3.72 mW·K^{-1} for the heat dissipation in such a steady-state measurement setup (see Fig. 3(a)). On this occasion, the ultrathin composite-caused small temperature change cannot be distinguished from the background signals. This phenomenon can be explained by simple heat transfer analyses. It is well established from 1D Fourier heat trans-

fer equation that heat flow $\dot{Q}$ is related to thermal conductive material cross-sectional area A and temperature gradient. For the nylon wire-supported measurement setup, the total heat flow is determined by the heat flow through sample $\dot{Q}_{\rm S}$, the heat flow through nylon wires $\dot{Q}_{\rm N}$ and the heat flow related to background leakage factors $\dot{Q}_{\rm B}$ (including conduction wires-relevant or thermocouples-correlated conduction heat flows and also the radiation heat flow), following the relationship

$$\dot{Q} = \frac{\kappa_{\rm S} A_{\rm S}}{L_{\rm S}} (T_{\rm h} - T_{\rm cS}) + \dot{Q}_{\rm B} + \frac{\kappa_{\rm N} A_{\rm N}}{L_{\rm N}} (T_{\rm h} - T_{\rm cN}).$$

The boundary condition can be described as $T_{\rm cS} = T_{\rm cN} = T_{\rm c} = T_0$, where T_0 is the room temperature. Meanwhile, $\dot{Q}_{\rm B}$ is identical for both the two setups. Thus, heat flow can be expressed as

$$\dot{Q} = \left(\frac{\kappa_{\rm S} A_{\rm S}}{L_{\rm S}} + \frac{\kappa_{\rm N} A_{\rm N}}{L_{\rm N}} \right) \Delta T + \dot{Q}_{\rm B},$$

$$\dot{Q} = \frac{\kappa_{\rm S} A_{\rm S}}{L_{\rm S}} \Delta T + \dot{Q}_{\rm B}$$

for measurement setups respectively with nylon wire supported and with hot junctions suspended. Owing to the ultra-thin sample nature, the nylon wire-induced heat flow portion is far larger than the sample-induced one, and thus scarcely any valid sample heat flow can be extracted from the obtained data when the hot junction is supported.

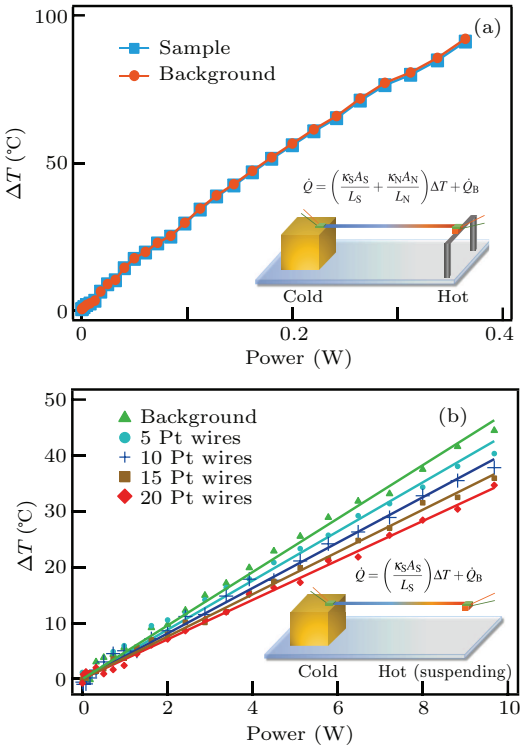


Fig. 3. Accuracy analyses for modified in-plane thermal conductivity measurement approach, showing (a) as-measured temperature variation results for the $(\rm MMT/rGO)_{10}$ composite from conventional steady-state measurement and (b) temperature differences between two junctions as a function of the heating power for different numbers of platinum wires. The solid line represents linear fitting results. The insets schematically illustrate the measurement setups with nylon wire-supported and suspended hot junctions, respectively.

Therefore, we, for the sake of measurement accuracy, determine to suspend the hot junction and the resulting background heat dissipation is reduced by an order of magnitude. To verify the measurement reliability, we use the modified method to measure the values of λ_x for different numbers of commercial platinum wires with diameters ~ 20 μm, whose thermal conductance is comparable to that of our tested ultra-thin composite film. The measurement results are shown in Fig. 3(b), and the background heat dissipation is also exhibited here. The calculated λ_x is 67.6 ± 6.7 $\rm W{\cdot}m^{-1}{\cdot}K^{-1}$, corresponding with its standard value of λ_x (72 $\rm W{\cdot}m^{-1}{\cdot}K^{-1}$). It is worth mentioning that there is a $\sim 2\%$ size distribution error (2% in length and 2‰ in cross-sectional area) between the purchased platinum wires, resulting in large measurement errors. On the other hand, the material property deviation from standard counterparts is also a main cause for λ_x different from standard result. This result further demonstrates the feasibility of this modified 1D steady-state heat conduction method to accurately determine the thermal conductivity of the materials with small thermal conductances.

2.3. Cross-plane thermal conductivity measurement

A modified 3ω method[28,29] is utilized to measure the cross-plane thermal conductivity (see Fig. 4(a)). The 10-mm-diameter composites are attached to a silicon substrate and a four-probe gold wire is patterned by using shadow mask and thermally evaporated on the composite film surface to form a 3ω testing structure. The main conducting path has a physical dimension of 1400 μm/30 μm as determined by gold wire length/width (see Fig. 4(b)). The SR830 lock-in amplifier provides an AC heating current for the gold wire and measures high-order harmonic voltage signals of the same wire to reflect thermal properties of composite film underneath it. A steady AC current I_ω with frequency ω is generated in the lock-in amplifier via the internal oscillator and V-to-I convertor, passing through two probes of the gold wire. The conducting gold wire is heated, and an oscillating heat flow enters into composite film. Depending on how fast heat enters into the film, an oscillating temperature $\Delta T_{2\omega}$ together with an oscillating electrical resistance can be measured on the wire via the other two voltage probes at an oscillation frequency of 2ω. The voltage oscillation $V_{3\omega}$ is eventually realized by combining the heat-induced resistance $R_{2\omega}$ with the current signal I_ω, and it is then detected with the lock-in amplifier on the same voltage probes to further extract the composite and substrate thermal properties. To ensure the measurement accuracy, a precise resistance box is connected in series into the circuit, and the intrinsic high-order harmonic noise is offset through a differential circuit. The supplied power remains constant for per unit wire length.

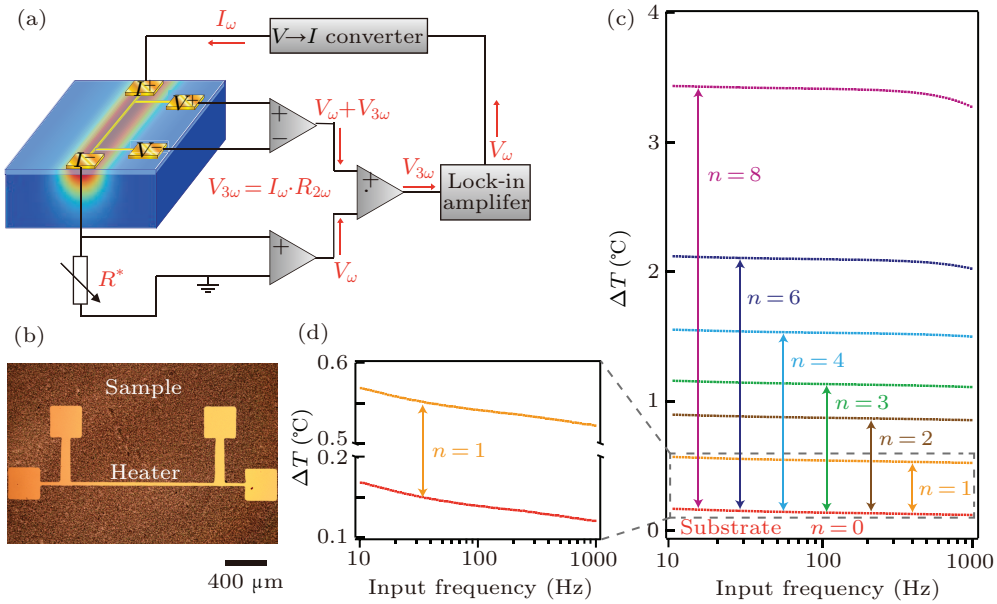


Fig. 4. (a) Schematic diagram of employed 3ω testing setup, (b) optical microscopy image for as-fabricated 3ω gold structure, (c) input frequency-dependent temperature oscillations for samples with various deposition cycles, and (d) enlarged view of temperature oscillation properties for substrate ($n=0$) and MMT/rGO/substrate ($n=1$).

Figures 4(c) and 4(d) show the gold wire's temperature oscillations against input current's frequency for samples with diverse deposition cycles. Experimental data are plotted in dots in different colors. Thermal characteristics of our samples can be extracted from the linear-region results based on an established approximate model,[30,31] where the slope reflects the substrate thermal properties while the temperature oscillation difference is related to composite λ_z. It is observed that the $\Delta T_{2\omega}$-logarithmic input frequency dependency deviates from the linear relationship in the high-frequency region, and this is a result of the gradually reduced thermal penetration depth approaching the film thickness. On the other hand, a similar phenomenon takes place in the low-frequency region due to the limited silicon substrate thickness. Furthermore, the linear-region slopes are all constant for tested composites with diverse values of n, meaning the fixed substrate thermal properties and further attesting our measurement accuracy. The calculated values of λ_z are 0.060, 0.066, 0.072, 0.069, 0.073, 0.058 W·m^{-1}·K^{-1} for composite films with deposition cycles of 1, 2, 3, 4, 6, and 8, respectively, while the silicon substrate possesses a typical conductivity value of 129.3 W·m^{-1}·K^{-1}. For comparison, we also measure the value of λ_z for pure rGO thin film and MMT thin film (thickness <1 μm) by using the same method. The obtained room-temperature λ_z value is 0.117 ± 0.016 W·m^{-1}·K^{-1} for rGO and 0.160 ± 0.022 W·m^{-1}·K^{-1} for MMT, consistent with the results reported previously.[4,32] Thus the measurement result accuracy and reliability are verified. Besides, we measure the values of λ_z of commercial SiO_2/Si wafers with diverse SiO_2 thickness values of 300 nm and 500 nm, and the derived values of λ_z are 130.43 ± 6.52 W·m^{-1}·K^{-1} and 1.47 ± 0.12 W·m^{-1}·K^{-1} for silicon substrate and oxide layer, respectively. These results also coincide well with the reported values.[31]

2.4. Thermal conductivity feature analysis

Thickness-related composite in-/cross-plane thermal conductivities are plotted in Fig. 5, where λ_x and λ_z values are denoted by using solid squares and solid circles, respectively. λ_x and λ_z are kept constant (3.99 ± 0.20 W·m^{-1}·K^{-1} and 0.066 ± 0.004 W·m^{-1}·K^{-1}) for composite films with various thickness values (*i.e.*, various values of deposition cycle n), meaning that the measured λ_x and λ_z values have very high accuracy. We also obtain the value of λ_x, 442.5 W·m^{-1}·K^{-1}, by using the laser flash method in Fig. 2(a). Apparently, significant difference can be seen between the two methods, showing that for determining the ultrathin composite film λ_x, the 1D steady-state heat conduction method is more accurate and effective than the laser flash method. These results also show that the composite films have a highly-anisotropic thermal conductivity, with an anisotropic ratio λ_x/λ_z being up to ~ 60.5 and independent of n. The obtained anisotropic ratio also has a high accuracy because the cross-plane thermal conductivity and the in-plane thermal conductivity measuring methods are both reliable. In view of the lack of reports on the thermal properties of ultrathin (<10 μm) composite films due to the difficulties in accurately evaluating their temperature variations, we compare our measurement results with those reported previously on thick composite counterparts with a thickness ranging from 10 μm to 10 mm. It is discovered that the measured value of λ_x (~ 3.99 W·m^{-1}·K^{-1}) is a common result for graphene/rGO-contained composite film,[26,33,34] and the high anisotropic ratio (~ 60.5) is also similar to that of MXene/MMT film,[24] demonstrating that

this proposed hybrid measuring method, instead of conventional laser flash technique, is greatly effective to accurately determine the anisotropic thermal counductivities of ultrathin composite films.

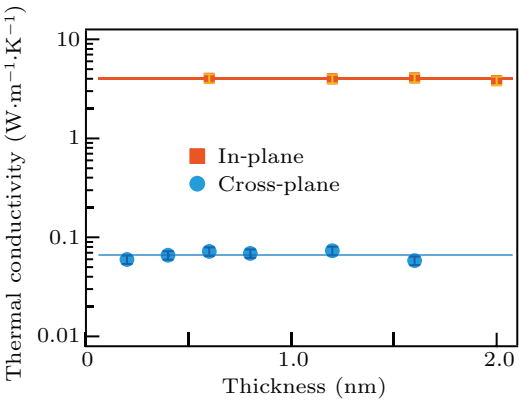


Fig. 5. Plots of thermal conductivity *versus* film thickness for $(MMT/rGO)_n$ composite.

3. Conclusions

In summary, we developed a hybrid method of determining ultrathin composite thermal conductivity , where a modified 1D steady-state heat conduction approach and a 3ω method are adopted to accurately assess its λ_x value and λ_z value, respectively. The obtained value of λ_x and λ_z are ~ 3.99 W·m^{-1}·K^{-1} and ~ 0.066 W·m^{-1}·K^{-1}, respectively, meaning the high anisotropic ratio of 60.5 for the tested ultrathin composite films. The thermal conductivity result is thickness-independent and close to that of reported thick composite counterpart, suggesting that the proposed method possesses a higher measurement accuracy than conventional techniques. This work presents a powerful guidance to measure the thermal properties of ultrathin composites, paving the way for developing the high-performance material towards efficient thermal management.

Acknowledgements

Project supported by the National Basic Research Program of China (Grant No. 2016YFA0200800), the Strategic Priority Research Program of Chinese Academy of Sciences (Grant Nos. XDB30000000 and XDB07030100), the Sinopec Innovation Scheme (A-527), the National Key Research and Development Program of China (Grant No. 2021YFA0715700), and the National Science Fund for Distinguished Young Scholars, China (Grant No. 52125302).

References

[1] Ball P 2012 *Nature* **492** 174
[2] Chu S and Majumdar A 2012 *Nature* **488** 294
[3] Prasher R 2006 *Proc. IEEE* **94** 1571
[4] Renteria J D, Ramirez S, Malekpour H, Alonso B, Centeno A, Zurutuza A, Cocemasov A I, Nika D L and Balandin A A 2015 *Adv. Funct. Mater.* **25** 4664
[5] Yang W, Zhao Z, Wu K, Huang R, Liu T, Jiang H, Chen F and Fu Q 2017 *J. Mater. Chem. C* **5** 3748
[6] Ma M, Xu L, Qiao L, Chen S, Shi Y, He H and Wang X 2020 *Chem. Eng. J.* **392** 123714
[7] Pan T W, Kuo W S and Tai N H 2017 *Compos. Sci. Technol.* **151** 44
[8] Hu D, Gong W, Di J, Li D, Li R, Lu W, Gu B, Sun B and Li Q 2017 *Carbon* **118** 659
[9] Zhao D, Qian X, Gu X, Jajja S A and Yang R 2016 *J. Electron. Packag.* **138** 040802
[10] Yan H, Yan J and Zhao G 2019 *Chin. Phys. B* **28** 114401
[11] Chen Q, Yan X, Wu L, Xiao Y, Wang S, Cheng G, Zheng R and Hao Q 2021 *ACS Appl. Mater. Interfaces* **13** 5435
[12] Li Q, Ma W and Zhang X 2016 *Int. J. Heat Mass Transfer* **95** 956
[13] Liu J, Wang H, Hu Y, Ma W and Zhang X 2015 *Rev. Sci. Instrum.* **86** 014901
[14] Lee B, Lee J S, Kim S U, Kim K, Kwon O, Lee S, Kim J H and Lim D S 2009 *J. Vac. Sci. Technol. B* **27** 2408
[15] Zhang Y F, Wang L, Heiderhoff R, Geinzer A, Wei B, Ji Y, Han X D, Balk L and Zhang Z 2012 *Chin. Phys. B* **21** 016501
[16] Xu X, Pereira L F, Wang Y, Wu J, Zhang K, Zhao X, Bae S, Tinh Bui C, Xie R and Thong J T 2014 *Nat. Commun.* **5** 3689
[17] Smith B, Vermeersch B, Carrete J, Ou E, Kim J, Mingo N, Akinwande D and Shi L 2017 *Adv. Mater.* **29** 1603756
[18] Takahashi C, Shirai T and Fuji M 2013 *Mater. Chem. Phys.* **141** 657
[19] Stobinski L, Lesiak B, Malolepszy A, Mazurkiewicz M, Mierzwa B, Zemek J, Jiricek P and Bieloshapka I 2014 *J. Electron Spectrosc. Relat. Phenom.* **195** 145
[20] Yu X, Zhang B, Zhao S, Kao Z, Yang S and Liu X 2018 *ECS J. Solid State Sci. Technol.* **7** M153
[21] Hsieh C T, Lee C E, Chen Y F, Chang J K and Teng H S 2015 *Nanoscale* **7** 18663
[22] Xu Y, Kraemer D, Song B, Jiang Z, Zhou J, Loomis J, Wang J, Li M, Ghasemi H, Huang X, Li X and Chen G 2019 *Nat. Commun.* **10** 1771
[23] Zhuang Y, Zheng K, Cao X, Fan Q, Ye G, Lu J, Zhang J and Ma Y 2020 *ACS Nano* **14** 11733
[24] Li L, Cao Y, Liu X, Wang J, Yang Y and Wang W 2020 *ACS Appl. Mater. Interfaces* **12** 27350
[25] Song N, Jiao D, Cui S, Hou X, Ding P and Shi L 2017 *ACS Appl. Mater. Interfaces* **9** 2924
[26] Song N, Jiao D, Ding P, Cui S, Tang S and Shi L 2016 *J. Mater. Chem. C* **4** 305
[27] Tian X, Itkis M E, Bekyarova E B and Haddon R C 2013 *Sci. Rep.* **3** 1710
[28] Qiu L, Zheng X, Yue P, Zhu J, Tang D, Dong Y and Peng Y 2015 *Int. J. Therm. Sci.* **89** 185
[29] Zheng X, Yue P, Li S, Wang L, Yang X and Chen H 2018 *Rev. Sci. Instrum.* **89** 084904
[30] Yamane T, Nagai N, Katayama S I and Todoki M 2002 *J. Appl. Phys.* **91** 9772
[31] Lee S M and Cahill D G 1997 *J. Appl. Phys.* **81** 2590
[32] Tiwari A, Boussois K, Ali B N, Smith D S and Blanchart P 2013 *AIP Adv.* **3** 112129
[33] Gong J, Liu Z, Yu J, Dai D, Dai W, Du S, Li C, Jiang N, Zhan Z and Lin C T 2016 *Composites Part A* **87** 290
[34] Ding P, Zhang J, Song N, Tang S, Liu Y and Shi L 2015 *Compos. Sci. Technol.* **109** 25